Cerebral Cortex September 2015;25:2729–2740
doi:10.1093/cercor/bhu070
Advance Access publication April 15, 2014

LSD1 Neurospecific Alternative Splicing Controls Neuronal Excitability in Mouse Models of Epilepsy

Francesco Rusconi[1,†], Leda Paganini[1,†], Daniela Braida[1], Luisa Ponzoni[1], Emanuela Toffolo[1], Annalisa Maroli[1], Nicoletta Landsberger[3,4], Francesco Bedogni[4], Emilia Turco[5], Linda Pattini[6], Fiorella Altruda[5], Silvia De Biasi[2], Mariaelvina Sala[1,7] and Elena Battaglioli[1,7]

[1]Department of Medical Biotechnology and Translational Medicine, [2]Department of Biosciences, Università Degli Studi di Milano, Milan 20122, Italy, [3]Theoretical and Applied Sciences, Division of Biomedical Research, University of Insubria, Busto Arsizio 21052, Italy, [4]San Raffaele Rett Research Center, Division of Neuroscience, San Raffaele Scientific Institute, Milan 20132, Italy, [5]Department of Molecular Biotechnology and Health Sciences, Molecular Biotechnology Center, Università Degli Studi di Torino, Turin 10126, Italy, [6]Dipartimento di Elettronica, Informazione e Bioingegneria-Politecnico di Milano, Milan, Italy and [7]CNR, Institute of Neuroscience, Milan, Italy

[†]Francesco Rusconi and Leda Paganini contributed equally to this work.

Address correspondence to Dr Elena Battaglioli, Department of Medical Biotechnology and Translational Medicine, Università degli Studi di Milano, Via Viotti 3/5, 20133 Milan, Italy. Email: elena.battaglioli@unimi.it

Alternative splicing in the brain is dynamic and instrumental to adaptive changes in response to stimuli. Lysine-specific demethylase 1 (LSD1/KDM1A) is a ubiquitously expressed histone H3Lys4 demethylase that acts as a transcriptional co-repressor in complex with its molecular partners CoREST and HDAC1/2. In mammalian brain, alternative splicing of LSD1 mini-exon E8a gives rise to neuroLSD1, a neurospecific isoform that, upon phosphorylation, acts as a dominant-negative causing disassembly of the co-repressor complex and de-repression of target genes. Here we show that the LSD1/neuroLSD1 ratio changes in response to neuronal activation and such effect is mediated by neurospecific splicing factors NOVA1 and nSR100/SRRM4 together with a novel *cis*-silencer. Indeed, we found that, in response to epileptogenic stimuli, downregulation of NOVA1 reduces exon E8a splicing and expression of neuroLSD1. Using behavioral and EEG analyses we observed that neuroLSD1-specific null mice are hypoexcitable and display decreased seizure susceptibility. Conversely, in a mouse model of Rett syndrome characterized by hyperexcitability, we measured higher levels of NOVA1 protein and upregulation of neuroLSD1. In conclusion, we propose that, in the brain, correct ratio between LSD1 and neuroLSD1 contributes to excitability and, when altered, could represent a pathogenic event associated with neurological disorders involving altered E/I.

Keywords: alternative splicing, epigenetics, epilepsy, Rett syndrome, transcription

Introduction

Alternative splicing represents a highly dynamic mechanism, which is emerging as a leading force toward proteome complexity. In mammalian nervous system, alternative splicing modulates pivotal processes such as synaptogenesis, neurite outgrowth, ion channel activity, and synaptic plasticity (Ule and Darnell 2006; Li et al. 2007). Recently, neurospecific splicing regulators have been discovered and studied in detail (Licatalosi and Darnell 2010; Irimia and Blencowe 2012). This group of RNA-binding proteins includes NOVA1/2, PTBP2/nPTB/brPTB, RBFOX1 (A2BP1), and the vertebrate-restricted nSR100 (SRRM4) (Boutz et al. 2007; Calarco et al. 2009). For instance, in response to neuronal depolarization, RBFOX1 exon 19 splicing is repressed, affecting both its subcellular localization and its splicing network (Lee et al. 2009). Also, NOVA splicing network can be modulated by neuronal activation in vivo through changes in the distribution of NOVA molecules between the nucleus and the cytosol. This process has been proposed to contribute to regulation of mRNAs and proteins associated with epilepsy (Eom et al. 2013).

However, apart from a few examples, the role of splicing mechanisms in activity-dependent brain plasticity remains unknown. Lysine-specific demethylase 1 (LSD1/KDM1A) is a transcriptional co-repressor that exerts its activity through demethylation of histone H3Lys4 and works in tight association with its co-repressors, CoREST and histone deacetylases HDAC1/2 (Shi et al. 2004; Forneris et al. 2005). The *LSD1* gene is highly conserved among vertebrates and contains 19 exons. In mammalian genomes, 2 additional exons, exon E2a and exon E8a are present allowing generation, by alternative splicing, of mammalian-restricted splicing variants (Zibetti et al. 2010). Interestingly, while exon E2a-containing isoforms can be found in all tissues, inclusion of the twelve-nucleotide long exon E8a is restricted to the nervous system, and generates 2 isoforms collectively indicated as neuroLSD1 (LSD1-8a and LSD1-2a/8a). NeuroLSD1 makes up a substantial proportion of total LSD1 mRNA in neurons, co-existing with and not substituting LSD1 (Zibetti et al. 2010). Alternatively, spliced exons coding for few amino acids may introduce post-translational modification sites that change protein function by preventing or permitting association with protein partners (Lipscombe 2005; Ellis et al. 2012). In fact, the second amino acid (Thr369b) of the 4 encoded by the alternatively spliced exon E8a can be phosphorylated (Toffolo et al. 2014). NeuroLSD1 phosphorylation transforms it into a weaker co-repressor unable to recruit HDAC activity, thus allowing transient increase in target gene transcription (Toffolo et al. 2014). On the other hand, LSD1 represents a strong, constitutive repressor whose activity is regulated by changes in its expression levels (Adamo et al. 2011). We previously showed that Thr369b phosphorylation is required for neuroLSD1 to modulate neuronal morphogenesis, highlighting the importance of alternative splicing in providing LSD1 with a molecular switch to derepress gene transcription (Toffolo et al. 2014). Consistently, we reported that, during the perinatal window, neuroLSD1 expression transiently increases becoming preponderant over LSD1 (Zibetti et al. 2010). These observations led us to hypothesize that also in adult brain LSD1/neuroLSD1 ratio could be

dynamically regulated in response to stimuli, thus contributing to brain plasticity.

Here, we describe how neuronal activity modulates neurospecific LSD1 splicing in vivo, causing a change in the LSD1/neuroLSD1 ratio, and dynamically regulating LSD1 activity in mammalian brain. We dissected the molecular mechanism controlling LSD1 alternative splicing in the brain and inferred the functional significance of LSD1 splicing modulation from the phenotype of neuroLSD1-null mice and *Mecp2*$^{y/-}$ mice, a genetic model of Rett syndrome. We found that neuroLSD1-null mice display a modified threshold of excitability as shown by reduced susceptibility to Pilocarpine-induced status epilepticus (PISE), whereas *Mecp2*$^{y/-}$ mice (Guy et al. 2001; Nan and Bird 2001) exhibit increased seizure susceptibility and neuroLSD1 overexpression. We suggest that, in this mouse model, NOVA1-mediated upregulation of neuroLSD1 levels could be causally linked to Rett syndrome-associated hyperexcitability.

Materials and Methods

Plasmids

Hybrid Minigene Constructs
Human genomic DNA was amplified to generate fragments containing the exon E8a along with its intronic flanking regions: MG-800 (chr1:23392283–23393062), MG-300 (chr1:23392283–23392629), and cloned into pBS-Splicing (Baralle and Baralle 2005). Flag-NOVA1 contains the human full-length cDNA (IMAGE IRATp970C06116D); Flag-nSR100 contains human full-length cDNA (Addgene, plasmid 35172).

Total RNA Extraction and RT-PCR Analysis
Total RNA was isolated using the Trizol reagent (Sigma-Aldrich, St Louis, MO, USA), and the purified RNA was treated with RNase-free DNase set (Qiagen, Valencia, CA, USA) to remove any residual DNA. Quantitative RT-PCR analysis was performed on an iQ5 Real-Time PCR Detection System (Biorad, Hercules, CA, USA) using the iScript™ two-step RT-PCR Kit with SYBR® Green (Biorad, Hercules).

Minigene Reporter Assay
The splicing assay was performed as described reporter plasmid (Baralle D and M Baralle 2005) in HeLa cells or SH-SY5Y. The MGs were transfected alone or together with 1:1 or 1:2 molar ratio relative to the expression plasmids pCMV-Flag-NOVA1 or Flag-nSR100.

Exon Inclusion Frequency by Relative Quantity Fluorescent-PCR (rqf-PCR)
Quantification was performed as described (Zibetti et al. 2010).

Generation of Exon E8a-Limited Knockout Mice
A mouse genomic clone, containing the region between exon 8 and exon 9 of m*LSD1*, was isolated from a 129Sv BAC clone bMQ374g24 using the recombeneering technique (Liu et al. 2003). The CRE-Neo cassette was inserted in an antisense orientation, in the ninth coding exon with the same recombeneering technique. The targeting vector was linearized at a unique Not I site. R1 ES cells were transfected with the targeting construct and selected in G418-containing media. Southern blotting with probe A of genomic DNA from 230 resistant clones showed that 2 of them had undergone homologous recombination. Positive clones were also analyzed with probe B and with a Neo-specific probe to confirm correct integration of the construct. Both clones were injected into C57Bl/6 blastocysts, and male chimeras displaying 100% agouti coat were mated to C57BL/6 and 129Sv females to produce outbred and inbred F1 heterozygous offspring. The described phenotypes were observed in mice derived from both ES cell clones. Mice were maintained and repeatedly backcrossed on C57BL/6 background for more than 10 generations. Routine determination of genotypes was performed by PCR with oligonucleotides derived from sequences flanking the targeted exon and from the Neo cassette.

Protein Extraction and Western Blotting
Tissues or cultured cells were homogenized essentially as described (Rusconi et al. 2010; Zibetti et al. 2010). Antibodies used: NOVA1 (Merk Millipore, Billerica, MA, USA) at 1:1000; CoREST (Upstate Biotechnology, Lake Placid, NY, USA) at 1:20 000; HA (Santa Cruz Biotechnology, Santa Cruz, CA, USA) at 1:1000; HDAC2 and HDAC1 (Abcam, Cambridge, UK); pan-LSD1 antibody (Diagenode, Liège, Belgium) at 1:10 000; TUBULIN (Cell Signaling, Danver, MA, USA) at 1:2000; GAPDH (Novus Biologicals, Littleton, CO, USA) at 1:2000.

Tissue Collection for Histology and Immunohistochemistry
Mice (9 knockout and 9 wild-type littermates at 8 weeks of age) were anesthetized and perfused with 4% paraformaldehyde in 0.1 M phosphate buffer (PB). After an overnight fixation in the same fixative at 4°C, brains were serially sectioned at 50 µm with a vibratome. Free-floating sections were either stained with thionin or with the fluorescent Nissl stain Neurotrace (Life Technologies, Carlsbad, CA, USA) for structural studies or subjected to immunohistochemistry with a 24 h incubation at room temperature. Used antisera are listed in Supplementary and Methods. Labeling was then visualized either with a standard avidin-biotin peroxidase method yielding a brown reaction product or with appropriate fluorescently labeled secondary antisera. Sytox green or 4′,6-diamidino-2-phenylindole (Life Technologies) were used to stain cell nuclei.

Chromatin Immunoprecipitation
Chromatin immunoprecipitation was performed as described (Stojic et al. 2011). Detailed description of the chromatin immunoprecipitation (ChIP) methodology together with primer sequences is present in the Supplementary Material section.

Experimental Animals and Chemicals
Male C57BL/6 wild-type and neuroLSD1 knockout mice of 5 or 16 weeks were used. All the experimental procedures followed the guidelines established by the Italian Council on Animal Care and were approved by the Italian Government decree No. 27/2010. Mice were individually housed throughout the testing period with free access to food and water at controlled temperature (20–22°C) with a 12-h light/dark cycle (lights on at 7:00 AM). The number of animals used and their suffering was minimized in all cases. All reagents were obtained from Sigma-Aldrich unless otherwise indicated. Analysis of behavioral seizure activity is described in details in Supplementary Material and Methods.

Results

NeuroLSD1 Splicing Variant is Transiently Downregulated During Status Epilepticus in Mice

To understand whether in adult brain LSD1/neuroLSD1 ratio could be dynamically regulated in response to experience, we used pilocarpine-induced status epilepticus (PISE) as a paradigm of neuronal activation. This pharmacological approach entails strong activation of hippocampal circuitry, where we show that LSD1 is highly expressed (Supplementary Fig. 1), and represents a model of human Temporal Lobe Epilepsy (Sharma et al. 2007). We treated 5-week-old C57BL/6 mice with pilocarpine (i.p.) using standard procedures (Shibley and Smith 2002) and performed behavioral observations addressing status epilepticus (SE), number, and severity of seizures according to the Racine scale (Racine et al. 1972). Mice were sacrificed 7 or 24 h after the onset of SE and total hippocampal RNA was extracted and retro-transcribed. LSD1 splicing isoform quantification was obtained by relative quantity fluorescence RT-PCR (rqfRT-PCR) (Zibetti et al. 2010). The alternative splicing

inclusion of E8a and/or E2a into LSD1 transcripts results in 4 possible different LSD1 isoforms (Fig. 1*A*, (Zibetti et al. 2010). To unambiguously evaluate all alternative splicing events, we used a single pair of primers amplifying all 4 isoforms. The amplicons were separated by capillary electrophoresis (electropherograms in Fig. 1*A*) and peak height was used for quantification (Fig. 1*B*,*C*). As shown in Figure 1*A*, 7 h after PISE both neurospecific isoforms containing exon E8a, neuroLSD1 (LSD1-8a and LSD1-2a/8a) were downregulated compared with control, whereas in parallel the ubiquitously expressed LSD1 isoforms (LSD1 and LSD1-2a) were increased. Notably, decrease of exon E8a-containing isoforms becomes detectable as soon as 4 h after the onset of seizures, reaching their lowest level at 7 h (Supplementary Fig. 2). Such change in the relative levels of the LSD1 isoforms was transient and by 24 h neuroLSD1 and LSD1 isoform levels were similar to controls. The histograms show the percentage of mature transcripts including exon E8a (Fig. 1*B*) or E2a (Fig. 1*C*) as average of 3 independent experiments. Overall LSD1 expression, measured by real-time quantitative PCR (qRT-PCR), did not change during the treatment (not shown) indicating that the observed neuroLSD1 downregulation was due to a reduction in exon E8a splicing frequency rather than to isoform-specific mRNA degradation. Importantly, activity-dependent downregulation was restricted to exon E8a splicing. In fact, inclusion of exon E2a was not changed upon PISE neither at 7 nor at 24 h after treatment, indicating that splicing repression was restricted to the neurospecific alternative exon (Fig. 1*C*).

NOVA1 Tunes NeuroLSD1 Levels in Response to Seizures by Regulating Exon E8a Splicing

In a previous in vivo study aimed at the identification of NOVA splicing regulatory network, LSD1 exon E8a has been reported to be physically associated with NOVA proteins (Zhang et al. 2010). To provide mechanistic evidence that NOVA1 regulates LSD1 neurospecific alternative splicing, we carried out minigene (MG) reporter assays. An 800 bp fragment including exon E8a and the highly conserved flanking intronic regions (hLSD1-MG800 in Fig. 2*A*) was cloned in the pBSplicing vector (Baralle et al. 2003), the resulting construct was transfected in SH-SY5Y and HeLa cells and exon E8a inclusion into MG mature transcripts was measured by rqfRT-PCR. As shown in Figure 2*A* in SH-SY5Y neuroblastoma cells exon E8a was included in about 13% of the MG mature transcripts whereas no inclusion was observed in HeLa cells, indicating that the cloned genomic sequence contains *cis*-acting elements required for neuron-restricted splicing. Co-transfection of hLSD1-MG800 along with increasing amount of NOVA1 showed a dose-dependent increase in exon E8a inclusion frequency in SH-SY5Y cells and no exon E8a inclusion in HeLa cells, even at the highest dose (Fig. 2*B*). These results indicate that, consistently with its ability to bind LSD1 transcripts (Zhang et al. 2010), NOVA1 actively participates in the regulation of exon E8a splicing.

Next, we asked whether NOVA1 could be responsible for the decrease in exon E8a splicing inclusion triggered by PISE. Seven hours after the onset of PISE, we purified the hippocampal proteins and assessed NOVA1 protein expression. As shown in Figure 2*C*, upon PISE, global NOVA1 protein levels, normalized over α-tubulin levels, were reduced by about 30%. This effect was not detectable at earlier time points (not shown), suggesting that it could be mediated by a reduction in the transcriptional rate. In parallel, the hippocampal RNA was purified and NOVA1 cDNA levels were evaluated by real-time qRT-PCR. As shown in Figure 2*D*, downregulation of NOVA1 protein levels correlated with a reduction of NOVA1 RNA levels which could already be measured 2 h after PISE (Supplementary Fig. 2). These results indicate that hippocampal NOVA1

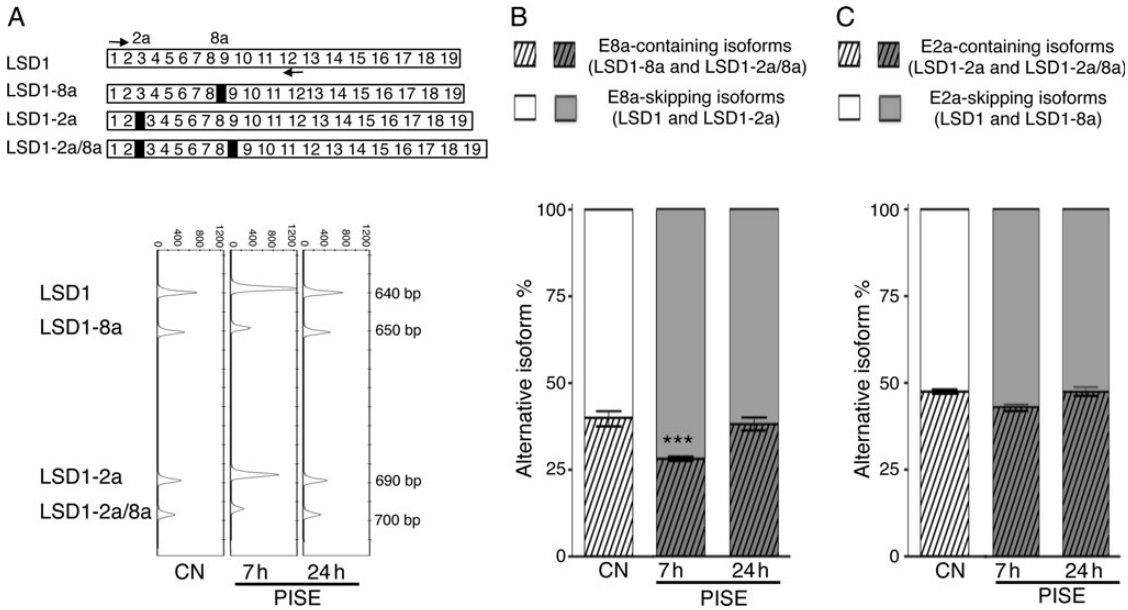

Figure 1. Neuronal activation in vivo induces LSD1 exon E8a splicing downregulation. PISE was elicited in 5-week-old C57BL/6 mice. Seven or 24 h after the onset of status epilepticus hippocampal RNA was analyzed ($n = 10$ mice per condition) and compared with control condition (CN). (*A*) Exon structure of the mammalian *LSD1* splicing isoforms. Arrows indicate and position of the primers used to identify transcripts characterized by the presence or absence of E2a and E8a. rqfRT-PCR electropherograms deriving from the amplification of endogenous LSD1 transcripts. In each electropherogram, different peaks represent the 4 LSD1 splicing variants. Amplicon size is indicated in bp. Quantification of peaks heights by GeneMapper software was used to calculate percentage of (*B*) E8a- or (*C*) E2a-containing isoforms relative to the sum of all the splicing variants. Results are shown as the mean ± SD. ***$P < 0.001$ assessed using Student's *t*-test. Asterisk referred to control condition (CN).

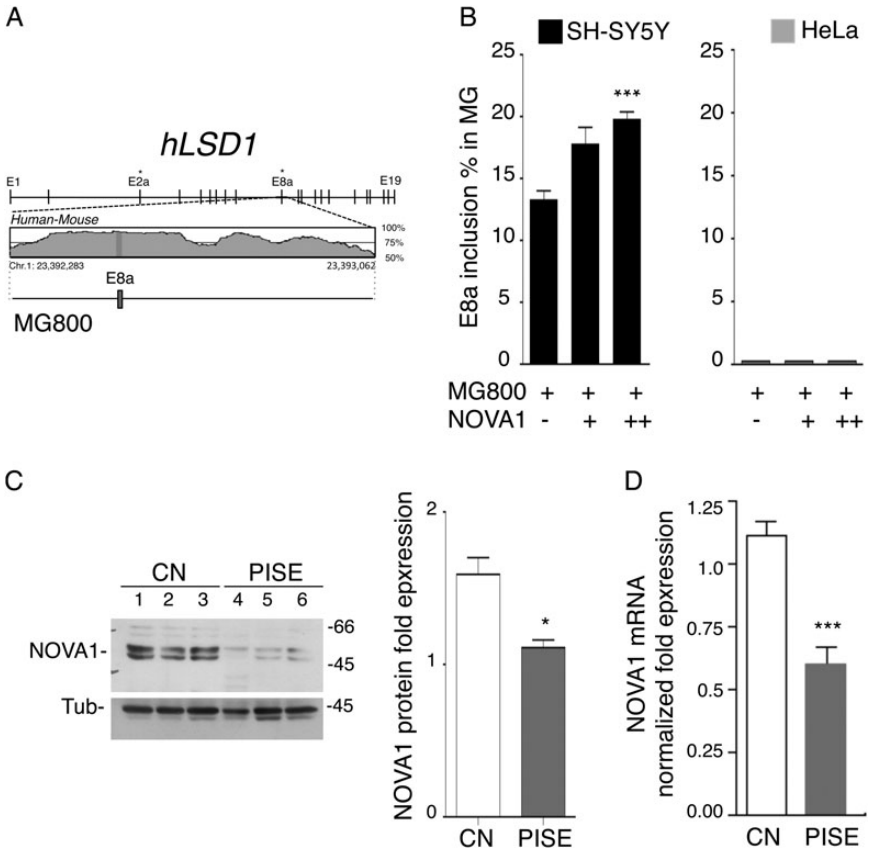

Figure 2. NOVA1 regulates exon E8a splicing inclusion and is responsible for neuroLSD1 sensitivity to neuronal activation. (*A*) Schematic representation of the human *LSD1* gene together with its exons ranging from 1 to 19; asterisks indicate the two alternative exons (E2a and E8a). Enlarged is the genomic region cloned into MG *hLSD1*-MG800. The "peaks and valleys" graph, obtained by Genome Vista browser, represents percentage conservation at given genomic coordinates between human and mouse LSD1 sequences. (*B*) Results of rqfRT-PCR testing exon E8a inclusion percentage in transcripts deriving from MG transfected in SH-SY5Y and HeLa cells in the presence of increasing amount of NOVA1 (+) or an empty vector (–). Peaks height obtained from GeneMapper software was used to calculate percentage of E8a-containing MG transcripts relative to the sum of all MG transcripts. Results are shown as the mean ± SEM. ***$P < 0.001$ assessed using ANOVA with post hoc Bonferroni's test. Asterisk is referred to the condition: MG800 (+) NOVA1 (–). (*C*,*D*) Hippocampal NOVA1 protein and mRNA expression in mice in response to pilocarpine (PISE) treatment compared with control (CN) ($n = 10$ mice per condition). (*C*) Total protein lysates from treated and control mice immunostained for NOVA1 and α-tubulin. Quantification of relative NOVA1 intensity (NOVA1/α-tubulin) is reported on the right. (*D*) NOVA1 mRNA expression level from treated and control mice normalized over RPSA mRNA level. Results are shown as the mean ± SEM. *$P < 0.05$; ***$P < 0.001$ assessed using Student's *t*-test.

transcription is sensitive to electrical activity and is downregulated in response to PISE. Altogether, these findings suggest that, NOVA1 downregulation in response to PISE could account for the concomitant reduction of exon E8a inclusion frequency into LSD1 mature transcripts.

NOVA1 and nSR100 Cooperate to Restrict Exon E8a Expression to the Nervous System

Our data indicated that NOVA1 is able to modulate exon E8a inclusion into MG-derived transcripts in a neuronal context but it is not sufficient to trigger splicing inclusion in HeLa cells, suggesting that NOVA1 is not directly responsible for restricting exon E8a splicing to the nervous system. In order to identify *cis*-acting elements regulating tissue-specific alternative splicing of LSD1 transcripts, we performed a deletion analysis. As shown in Figure 3*A*, deletion of the 450 bp located at the 3′ (hLSD1-MG350) resulted in a dramatic increase of exon E8a inclusion in SH-SY5Y (up to 70% of the mature MG transcripts), indicating the presence of a strong negative *cis*-acting element within the removed fragment. By computer-assisted analysis of the deleted region, we identified a palindromic 21-bp element containing the reverse complement of exon E8a (Supplementary Fig. 3). This palindrome is 100% conserved among mammals and maps about 300 bp downstream of exon E8a. Given its perfect complementarity to exon E8a, at the pre-mRNA stage, this region could trap the mini-exon and its donor and acceptor splicing sites into a perfect 21-bp-long double-stranded RNA structure (Supplementary Fig. 3*B*,*C*) hampering the splicing process. Consistently, as shown in Figure 3*A*, deletion of the 12-bp core sequence complementary to exon E8a from the palindrome (hLSD1-MG800Δpal) resulted in a massive increase of exon E8a inclusion (85% of total MG transcripts). These data suggest that the palindromic element acts as a *cis*-silencer of exon E8a splicing in neuronal cells. However, as removal of this element was not sufficient to allow exon E8a inclusion in HeLa cells (Fig. 3*A*), our results also indicate that, besides NOVA1, another neurospecific *trans*-acting factor is required to trigger E8a splicing. In order to identify it, we selected a small subset of tissue-specific RNA binding factors (Braunschweig et al. 2013), namely nPTB, RB-FOX1, SAM68, and nSR100, and tested each of them for capability to drive exon E8a inclusion in non-neuronal cells (not shown). We found that, in HeLa cells, overexpression of

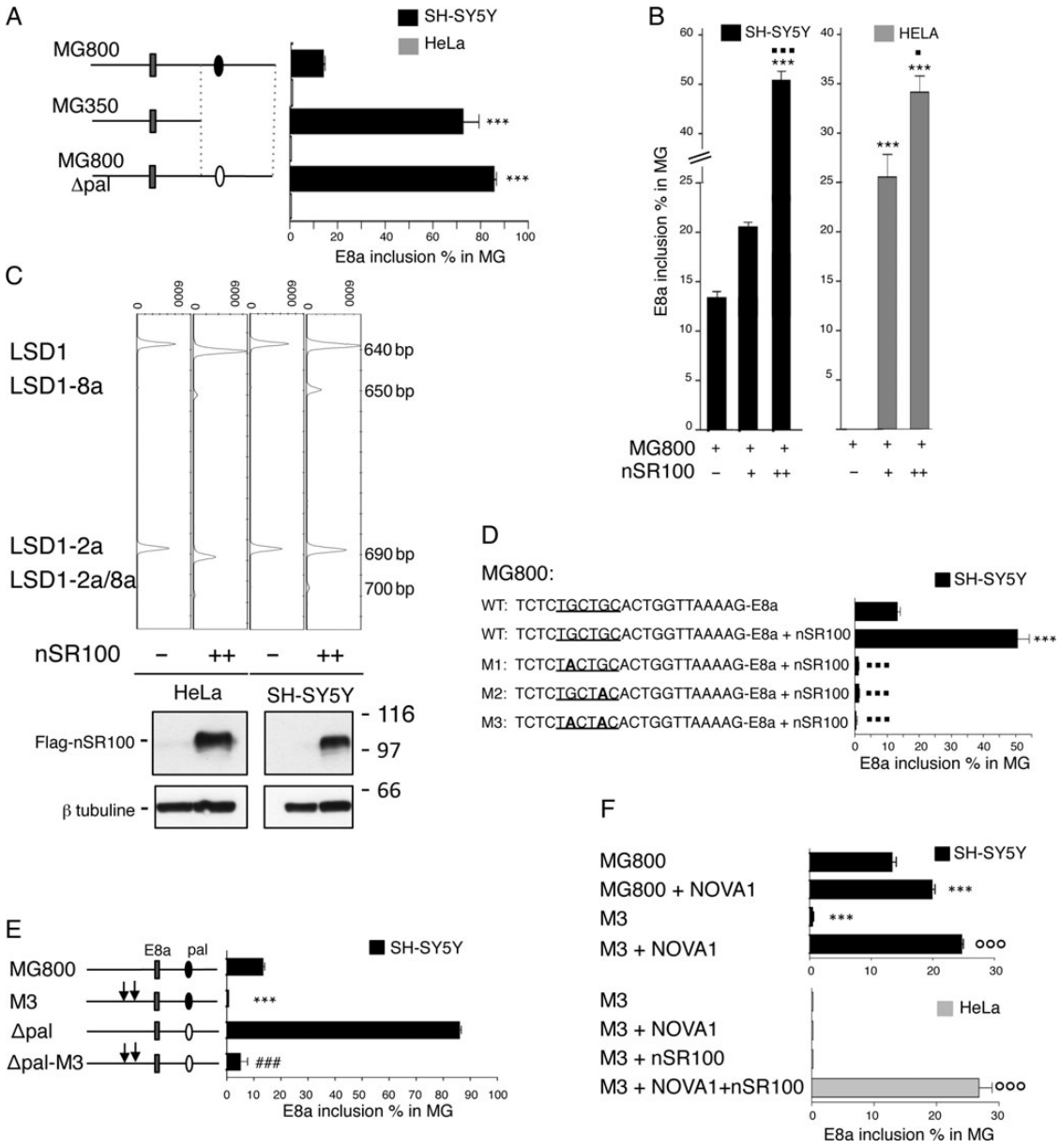

Figure 3. nSR100 positively regulates exon E8a alternative splicing while a *cis*-acting palindromic sequence acts as negative regulator. (*A*) Quantification of exon E8a inclusion frequency in mature *hLSD1*-MGs transcripts from transfected SH-SY5Y and HeLa cells. Different *hLSD1*-MG plasmid names indicate bp of the cloned human *LSD1* genomic region. Rectangle indicates exon E8a, full oval symbol indicates the palindromic sequence, the empty one its deletion. Note that inclusion in HeLa cells is zero in all conditions. (*B*) Quantification of exon E8a inclusion frequency in SH-SY5Y and HeLa cells transfected with MG800, plus nSR100 (+) or an empty vector (−) at 2 different doses. (*C*) Human LSD1 isoform expression from Hela and SH-SY5Y transfected with nSR100 (++) or an empty vector (−). (*D*) Quantification of exon E8a inclusion frequency in SH-SY5Y transfected with *hLSD1*-MG800 or with nSR100 and *hLSD1*-MG800 carrying single (M1 and M2) or double mutations (M3). (*E*) Quantification of exon E8a inclusion frequency in SH-SY5Y transfected with the wild-type or mutant (M3) MG800, including or not (Δpal) the palindromic region. Vertical arrows indicate the mutated bases of nSR100 binding site. (*F*) Quantification of exon E8a inclusion frequency in SH-SY5Y transfected with the wild-type or mutant (M3) MG800 together with NOVA1. (*A*–*F*) Percentage of E8a-containing MG transcripts was calculated as described in Figure 1. Results are shown as the mean ± SEM. Statistical analysis: one-way ANOVA with post hoc Bonferroni's test. ***, ■■■, ###, ○○○ for $P < 0.001$; ■$P < 0.05$. Asterisk is referred to MG800; filled box MG800 +nSR100; hash to MG800 Δpal; open circle to MG800-M3.

the SR protein nSR100 (also known as SRRM4) promoted exon E8a inclusion not only into MG hLSD1-MG800 transcripts (Fig. 3*B*), but also into endogenous LSD1 transcripts, in a dose-dependent manner (Fig. 3*C*). As expected, in SH-SY5Y overexpression of nSR100 was able to strongly increase exon E8a inclusion into MG hLSD1-MG800 reporter transcripts and into endogenous ones. These results collectively indicate nSR100 as the necessary and sufficient factor regulating LSD1 neuro-specific splicing. It is known from the literature that direct interaction between nSR100 and the pre-mRNA targets is necessary to promote exon inclusion and is mediated by conserved UGC motifs upstream of the splice acceptor site of the nSR100-regulated exons (Nakano et al. 2012). We identified a UGCUGC sequence 12 bp upstream exon E8a, which is 100% conserved among mammals (Supplementary Fig. 4). As shown in Figure 3*D*, we found that introduction of a single- or a double-nucleotide substitution into nSR100 consensus sequence previously shown to abrogate nSR100 binding to RNA

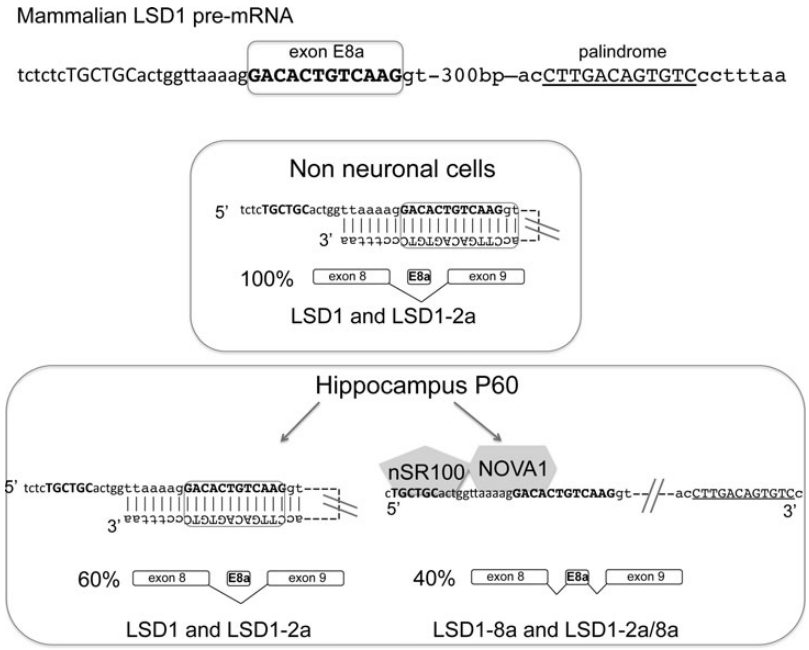

Figure 4. Schematic model recapitulating exon E8a splicing regulation by *cis*- and *trans*-acting factors. In bold exon E8a sequence, underlined the palindrome "12 bp core." In capital letters, nSR100 consensus binding sequence. In non-neuronal cells where neurospecific splicing factors are absent, exon E8a is never included. In neuronal cells, NOVA1 and nSR100 binding to LSD1 pre-mRNA promote splicing inclusion but have to counteract palindrome annealing to exon E8a in order to expose E8a donor and acceptor splicing sites. We hypothesize that, in neuronal cells, the presence of the palindrome ensure a fine balance between neuronal and non-neuronal isoforms: for instance, in P60 mouse hippocampus, the ratio between neuronal and non-neuronal isoforms is, respectively, 60% and 40%. In non-neuronal cells, palindrome represents an intrinsic safe lock mechanism to avoid aberrant E8a splicing inclusion.

(Nakano et al. 2012) completely abolished not only the effect of nSR100 overexpression on exon E8a inclusion but also the exon E8a inclusion observed in SH-SY5Y cells in basal conditions, when nSR100 is not overexpressed. This suggests that basal exon E8a inclusion into MG transcripts is due to the low level of expression of the endogenous nSR100 gene observed in SH-SY5Y (not shown).

To summarize, our data indicate that 3 key elements are responsible for regulating expression of neuroLSD1 in neuronal cells, a palindromic *cis*-acting negative regulator and 2 *trans*-acting neurospecific splicing factors, nSR100 and NOVA1. To investigate the functional interplay between these elements, we generated a construct (hLSD1-MG800Δpal-M3) lacking both the palindrome and the nSR100 consensus sequences. As shown in Figure 3*E*, removal of the palindrome when nSR100 consensus sequences are not present did not increase exon E8a splicing in SH-SY5Y, suggesting that the palindrome acts by antagonizing nSR100 activity and its removal is not able per se to promote splicing, in agreement to the data obtained in HeLa cells (Fig. 3*A*).

Next, we analyzed the functional relationship between the 2 *trans*-acting factors, NOVA1 and nSR100, by measuring the effect of NOVA1 overexpression on exon E8a splicing when nSR100 binding sequences are mutated. Surprisingly, we found that, in SH-SY5Y (Fig. 3*F*), NOVA1 overexpression was able to restore exon E8a inclusion into hLSD1-MG800-M3 transcripts even when nSR100 binding sites are missing. Importantly, in HeLa cells, NOVA1 alone is not sufficient to rescue exon E8a inclusion in hLSD1-MG800-M3-derived transcript, but requires nSR100 co-transfection (Fig. 3*F*). This result indicates that NOVA1 and nSR100 cooperate to bind LSD1 pre-mRNAs. Furthermore, performing co-immunoprecipitation experiments using overexpressed HA-NOVA1 and Flag-nSR100, we found that the 2 proteins are part of the same splicing-regulating complex (Supplementary Fig. 5).

Taken together, these results indicate that nSR100 and NOVA1 and the *cis*-acting palindrome cooperate in restricting neuroLSD1 expression to the nervous system. Importantly, we found that nSR100 levels were not affected by neuronal activation (Supplementary Fig. 4*B*), suggesting that changes in NOVA1 protein levels are sufficient to finely tune exon E8a splicing in response to electrical activity in the hippocampus. A schematic model for regulation of exon E8a by *cis*- and *trans*-acting factors is illustrated in Figure 4.

Generation of NeuroLSD1-Null Mice

In order to understand the physiologic relevance of exon E8a in normal and pathological responses in the CNS, we generated a gene targeting mutant mouse line specifically ablating exon E8a, to obtain a neuroLSD1 knockout (neuroLSD1^{KO}). Standard homologous recombination procedures were employed to ablate the 12 nucleotides long exon E8a without interfering with the expression of the *LSD1* gene and with the production of the ubiquitously expressed LSD1 splicing isoforms (Fig. 5*A*,*B*). Two independent ES cell clones were isolated carrying the correct homologous recombination event (Fig. 5*B*). Heterozygous mice were backcrossed at least 8 times on C57BL/6 background and congenic breeding was estimated (not shown). Homozygous mutants and control wild-type littermates were obtained by crossing heterozygous animals. The frequency at birth of the different genotypes obtained from intercrossings was consistent with Mendelian inheritance. Lack of neuroLSD1 (LSD1-8a and LSD1-2a/8a) expression and

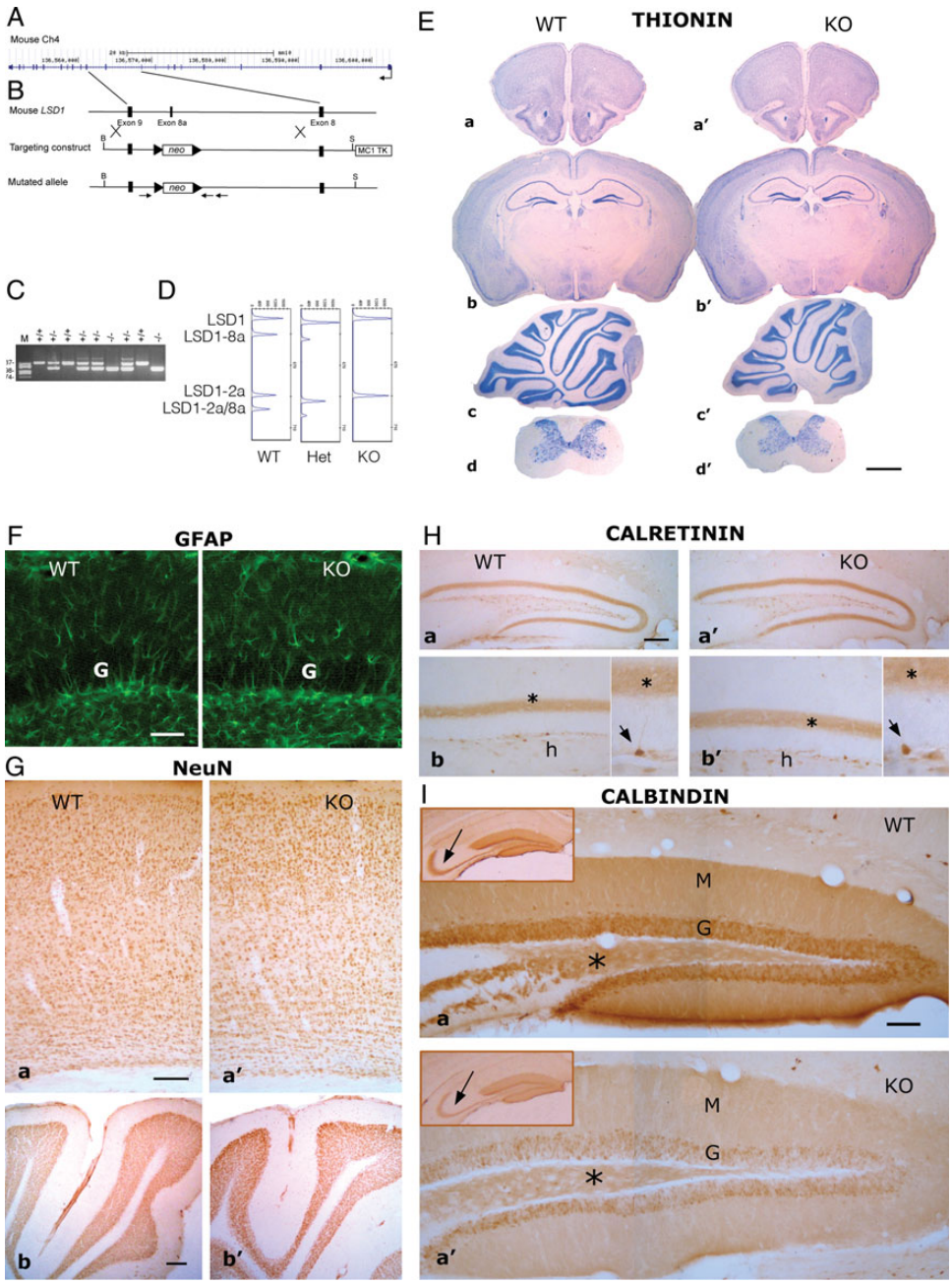

Figure 5. Brains lacking neuroLSD1 retain LSD1 expression and display normal morphology. (*A*) Schematic representation of mouse *LSD1* gene. (*B*) Exon *E8a* deletion strategy: targeting construct and mutated allele are shown. (*C*) PCR genotyping with primers F1, R1, and R2 on a representative litter of neuroLSD1 +/−. (*D*) rqfRT-PCR analysis of hippocampal RNA from wild-type, heterozygous, and knockout animals. (*E–I*) Brain cytoarchitectural analysis of wild-type and knockout adult mice. (*E*) Photomicrographs of thionin-stained vibratome sections; a, a′, coronal section at the level of frontal cortex and anterior olfactory nuclei; b, b′, coronal section at the level of somatosensory cortex, hippocampus, and diencephalon; c, c′, sagittal section of cerebellum; d, d′, transverse section of spinal cord. Scale bars = 1.3 μm for a–b′; 1.9 μm for c–d′. (*F*) Immunostaining for GFAP in the hippocampus; G = granule cell layer of dentate gyrus; Scale bar = 160 μm. (*G*) Immunostaining for NeuN in the cerebral cortex a, a′ and cerebellum b, b′. Scale bars = 370 μm. (*H*) Immunostaining for calretinin in the hippocampus; a, a′; b–b′, labeled neurons are in the hilus (h) and subgranular zone (arrowheads) and labeled terminals form a band in the inner molecular layer (asterisks); Scale bars = 940 μm for a, a′; 370 μm for b, b′. (*I*) Immunostaining for Calbindin in the hippocampus; a, a′; G = granule cell layer, M = molecular layer of dentate gyrus; asterisks denotes mossy fibers in the hilus. Low power inserts show the mossy fibers projections to the CA3 region (arrows); Scale bars = 170 μm, inserts 600 μm.

retention of ubiquitous LSD1 (LSD1 and LSD1-2a) expression was assessed by rqfRT-PCR in hippocampus (Fig. 5*D*) and different brain areas (not shown). Importantly, LSD1 levels were assessed both at RNA and at protein levels in hippocampus using pan-LSD1 real-time qRT-PCR primers as well as pan-LSD1 antibody (Supplementary Figs 6 and 7). As expected, total LSD1 expression in neuroLSD1^{KO} mice (expressing only the ubiquitous LSD1) was comparable with that observed in wild-type mice.

Animals were healthy and did not show any alteration of the vital parameters: weight, dimensions, and fertility were unaffected by the mutation and no morphological defects were detected (Fig. 5*E* and Supplementary Fig. 8). Immunohistochemistry showed a normal pattern of labeling with anti-GFAP (glial

fibrillar acid protein, a marker of astrocytes), indicating absence of astroglial activation (Fig. 5*F*) and with anti-NeuN (neuronal nuclear antigen, a pan-neuronal marker), indicating absence of abnormalities in neuronal distribution and density (Fig. 5*G*). In the hippocampus, the immunostaining for the calcium binding protein Calretinin was normal (Fig. 5*H*), whereas a weaker immunostaining for the calcium binding protein Calbindin was evident in the hippocampus dentate gyrus and CA3 of neuroLSD1^{KO} mice compared with wild-type littermates (Fig. 5*I*). Decreased Calbindin protein levels were not accompanied by mRNA variations as revealed by qRT-PCR experiments from hippocampal tissues (not shown).

Immunohistochemical localization of LSD1 using a pan-LSD1 antibody showed an identical pattern and intensity of labeling in all brain sections of wild-type and neuroLSD1^{KO} mice analyzed (Supplementary Fig. 7). Finally, also the immunoreactivity for the LSD1 dimethylated substrates H3K4 and H3K9 was unaffected in neuroLSD1^{KO} mice compared with wild-type littermates (Supplementary Fig. 6).

Lack of NeuroLSD1 Strongly Attenuates Seizure Susceptibility

To investigate the physiological significance of the neuroLSD1 downregulation observed in wild-type mice upon PISE (Fig. 1), we applied the same paradigm to neuroLSD1^{KO} mice (Fig. 6). The behavioral response to PISE was monitored over one and a half-hour period after pilocarpine administration in 5-week-old neuroLSD1^{KO} mice and wild-type littermates (Fig. 6*A*). Different behavioral aspects were considered, including number of animals undergoing SE, number of convulsive events occurring during SE, latency to seizure and lethality. All these parameters revealed a substantial reduction in seizure susceptibility of neuroLSD1-null mice relative to wild-type littermates.

To further characterize PISE susceptibility of both genotypes, we examined their EEG profile. To establish the EEG baseline, continuous 16-h (from 17.00 PM to 9.00 AM) video-EEG recordings were obtained from 5 conscious, unrestrained, 4-month-old neuroLSD1^{KO} mice and 5 wild-type littermates. Sixteen-hour EEG traces from a neuroLSD1^{KO} and a wild-type mouse (Fig. 6*B*) revealed similar pattern. No significant difference in mean amplitude and spike activity was found between wild-type and neuroLSD1^{KO} mice (Fig. 6*B*). The mean spectral power distribution, evaluated every hour, did not significantly differ between the 2 genotypes.

Pilocarpine injection induced different EEG pattern in both genotypes as shown by two representative EEG traces in Fig. 6*C*. The wild-type mice showed trains of spikes followed by voltage attenuation, while the neuroLSD1^{KO} showed spindle-like events. Rhythmic spindle-like activity (absence, stage 1) was observed in 22% of wild-type and 54% of neuroLSD1^{KO} mice, and train of spikes (tonic–clonic seizures: stage 4–5) in 78% of wild-type and 46% of neuroLSD1^{KO}, during the first hour after pilocarpine injection (Fig. 6*C*). NeuroLSD1^{KO} mice were less prone to PISE as shown by the lack of mean amplitude increase during the second hour (Supplementary Fig. 9). Only 26% of the KO animals died, in contrast to 78% of wild-type mice. Altogether, these results indicate that, while in resting conditions, neuroLSD1^{KO} mice are indistinguishable from wild-type littermates, they display a clear protection toward pharmacologically induced abnormal neuronal activation. This phenotype suggests that neuroLSD1 controls neuronal excitation in mammalian brain.

NOVA1 Upregulation in the Mecp2$^{y/-}$ Mouse Model Affects NeuroLSD1 Splicing

Conditions in which NOVA1 levels and activity are altered have already been described. For instance, it has been shown that NOVA1 levels (Jelen et al. 2010) and subcellular localization (Eom et al. 2013) are modulated in the brain in response to PISE. Intriguingly, Zoghbi and colleagues listed NOVA1 as a negatively regulated MeCP2 target (Ben-Shachar et al. 2009). Mutations in the methylated cytosine binding protein MeCP2 cause Rett syndrome, a disease characterized by epilepsy in 80% of the patients (Guy et al. 2011; Dolce et al. 2013). *Mecp2$^{y/-}$* mice represent the most studied animal model to get into RTT physiopathology as they recapitulate several aspects of the human disease, including the epileptic phenotype (Guy et al. 2001). We therefore asked whether NOVA1 is upregulated in a *Mecp2$^{y/-}$* mice and consequently whether also neuroLSD1 is affected in this model. Hippocampal NOVA1 transcripts obtained from P40 *Mecp2$^{y/-}$* (Guy et al. 2001) and control littermates, quantified by qRT-PCR (Fig. 7*A*), were found significantly upregulated in mutant mice. Consistently, also NOVA1 protein was upregulated as shown by western blot analysis (Fig. 7*B*). These data well fit with a model in which MeCP2 binds and negatively regulates NOVA1 transcription. Therefore, we performed ChIP with anti-MeCP2 antibody using hippocampal tissues to verify whether we could detect an enrichment of MeCP2 binding to the NOVA1 promoter in vivo. By quantitative qRT-PCR, we detected a significant enrichment of MeCP2 binding to NOVA1 promoter region compared with mock condition. Binding specificity to NOVA1 promoter was assessed addressing MeCP2 occupancy of the *CDKl4* promoter that has already been considered a nontarget of MeCP2 (Chahrour et al. 2008); as second negative control, we used the *Egr1* promoter whose transcription, to the best of our knowledge has never been found affected by MeCP2 (Fig. 7*C*). Although we are aware that, in neurons, MeCP2 is so abundant to be globally bound (Skene et al. 2010), we suggest that our data indicate that in the hippocampus MeCP2 might have a stronger association with the regulatory regions of NOVA1 therefore permitting to obtain the identified regulation in *Mecp2*-null mice.

Since NOVA1 affects LSD1 splicing, to further confirm the above results we proceeded using rqfRT-PCR to assess exon E8a inclusion frequency in RNAs extracted from hippocampus, cerebellum and cortex of *Mecp2$^{y/-}$* and control mice (Fig. 7*D*). As expected, a significant upregulation of neuroLSD1 isoforms accompanied by a corresponding decrease in the ubiquitous LSD1 isoforms was detected in all brain areas of *Mecp2$^{y/-}$* analyzed compared with wild-type littermates. Again, alternative splicing of LSD1 exon E2a, the ubiquitous alternatively spliced exon, did not change in any region (not shown).

Discussion

In the present study, we describe how neuronal activity controls the neurospecific splicing of the epigenetic co-repressor LSD1 in mammalian nervous system. We show that inclusion of the E8a mini-exon into LSD1 mature transcripts is sensitive to neuronal activity and we provide evidence indicating that

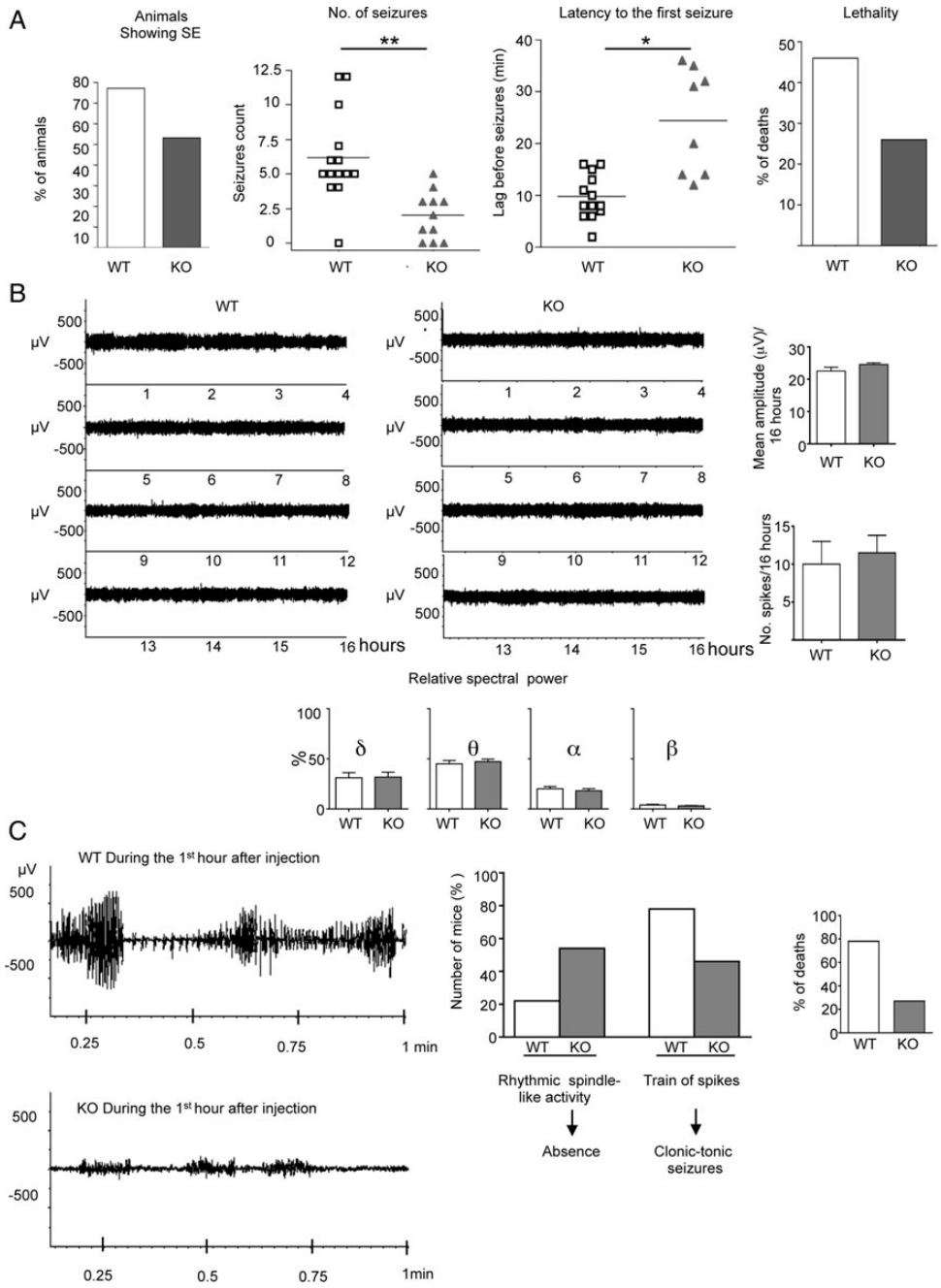

Figure 6. Behavioral and electroencephalographic analysis of wild-type (WT) and neuroLSD1^{KO} (KO) mice susceptibility to PISE. (*A*) Behavioral analysis were conducted in 5-week-old mice ($n = 11$–13 mice per genotype) treated with pilocarpine (270 mg/kg i.p.). Continuous observation has been performed over 1.5 h after injection. From the left to the right: Percentage of mice which undergo Status Epilepticus; number of stage 5 tonic–clonic seizures experienced; time lag between pilocarpine i.p. injection and the first stage 5 tonic–clonic seizure event; pilocarpine-induced lethality. Number and latency to seizures are shown as the mean ± SEM. $^{*}P < 0.05$; $^{**}P < 0.01$ assessed using Student's *t*- test. (*B*) Electroencephalographic analysis was conducted in 3-month-old mice ($n = 9$–11 mice per genotype). A 16-h representative EEG trace of one wild-type and one neuroLSD1^{KO} mouse. In small histograms, mean amplitude, spike activity, and relative spectral power are quantified between wild-type and neuroLSD1^{KO} mice. (*C*) Effect of pilocarpine (270 mg/kg i.p.) on EEG evaluated for 1 h after injection. Left: Representative trace of 1-min recording from a wild-type mouse showing a generalized tonic–clonic seizure (upper) and from a neuroLSD1^{KO} mouse showing rhythmic spindle-like activity associated with an absence seizure (bottom). Centre: Different seizure pattern exhibited by wild-type and knockout mice. Right: Lethality of mice receiving pilocarpine evaluated until 7 days.

the resulting neuroLSD1 isoform is a key factor contributing to in vivo modulation of neuronal excitability. In neurons, alternative splicing is instrumental to the proteome reprogramming underlying cellular response to stimuli. Alternative splicing of several synaptic factors such as ion channels, and receptors (Li et al. 2007; McKee and Silver 2007; Kalsotra and Cooper 2011; Eom et al. 2013) has been described to be affected by neuronal activation. Recently, the neurospecific splicing modulator NOVA has been shown to be modified by excitatory cues, suggesting a role for this RNA-binding protein in the splicing pattern changes triggered by neuronal activity (Eom et al. 2013). We found that in mouse hippocampus response to PISE entails NOVA1 downregulation at RNA and protein level and a concomitant decrease in LSD1 neurospecific

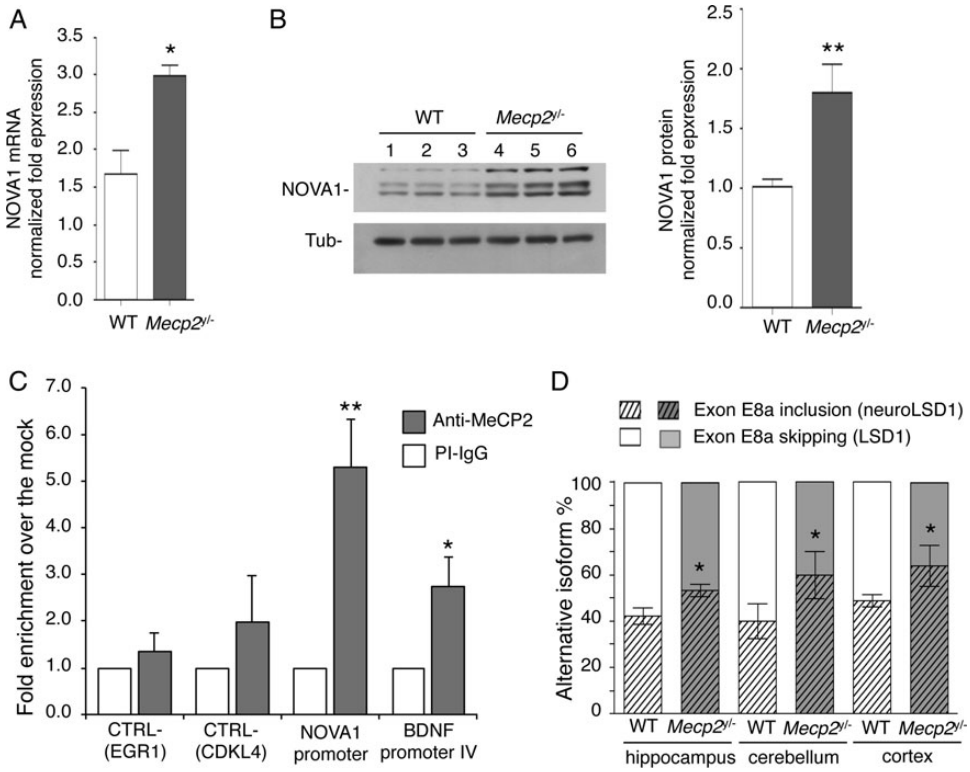

Figure 7. NOVA1 is a downstream target of MeCP2 and is upregulated in hippocampus of *Mecp2*$^{y/-}$ mice. (*A*) NOVA1 mRNA expression level in wild-type versus *Mecp2*$^{y/-}$ mice normalized over RPSA expression. (*B*) NOVA1 immunoblot analysis of total hippocampal protein extracts from wild-type (WT) and *Mecp2*$^{y/-}$ littermates. Densitometric quantification of relative NOVA1 intensity (NOVA1/α-Tubulin) is reported on the right. (*C*) MeCP2 chromatin occupancy to the promoter region of NOVA1, BDNF promoter IV or two unrelated promoters, Egr1 and CDKl4, analyzed by quantitative qRT-PCR. Values are normalized over the input and expressed as relative enrichment over preimmune serum (mock condition). (*D*) LSD1 neurospecific splicing is upregulated in *Mecp2*$^{y/-}$ mice compared with wild-type littermates. Histograms represent LSD1 isoforms relative percentage in hippocampus, cerebellum and cortex. ($n = 5$–6 mice per genotype). Results are shown as the mean ± SEM. *$P < 0.05$; **$P < 0.01$ assessed using Student's *t*-test.

splicing. Using a MG splicing-reporter assay we demonstrate that NOVA1 positively modulates exon E8a splicing inclusion generating the neuroLSD1 isoform, thus establishing a causal link between NOVA1 decrease and neuroLSD1 downregulation. Importantly, it has been proposed that reduction of NOVA1 activity within the nucleus in response to PISE can result in homeostatic proteomic remodeling able to transiently modify hippocampal threshold of excitability to prevent further seizures (Eom et al. 2013). Since NOVA1 controls LSD1 neurospecific splicing, we hypothesized that the neuroLSD1 downregulation triggered by PISE could represent a transcriptional-based homeostatic mechanism mediating neuronal adaptive response to status epilepticus. To test this hypothesis, we generated exon *E8a*-restricted null mice. The behavioral studies as well as EEG recordings we report indicate that neuroLSD1-null mice, although indistinguishable from wild-type littermates in resting conditions, are protected from pharmacologically induced status epilepticus and exhibit a remarkably diminished seizure susceptibility.

Moreover, we show that in *Mecp2*$^{y/-}$ mice, a model of human RTT syndrome characterized by neural circuits hyperexcitability and recurrent seizures (Zhang et al. 2008; Shepherd and Katz 2011), both neuroLSD1 and NOVA1 are upregulated. NOVA1 has been reported to be downregulated in a *MECP2*-Tg mouse model (Chahrour and Zoghbi 2007; Chahrour et al. 2008), and based on this finding has been suggested to be a target of *MECP2*. Consistently, here we show that NOVA1 is upregulated in the *Mecp2*-null mice and we demonstrate, by ChIP, that MeCP2 is associated with NOVA1 promoter in vivo, providing more direct evidence supporting the role of NOVA1 as target of MeCP2-negative regulation.

Altogether, our investigations into the mechanism underlying the effect of neuronal activity on the neurospecific splicing of LSD1 led us to the identification of 3 elements involved: 2 neurospecific splicing factor, NOVA1 and SR-protein nSR100, acting as positive *trans*-acting factor restricting exon E8a inclusion specifically to neurons, and a palindromic region that functions as negative *cis*-acting splicing regulator ubiquitously blocking default splicing. These results show how evolution selected a very effective strategy to prevent LSD1 neurospecific splicing outside the nervous system and to tightly regulate neuroLSD1 levels within the CNS in response to neuronal activation.

A consistent body of evidence emphasizes the relevance of the transcription factor REST in transcriptional control of circuitry excitability, in particular through its ability to repress specific genes in the nervous system (Garriga-Canut et al. 2006; Roopra et al. 2012). LSD1 is a well-characterized co-repressor actively contributing to repress REST targets (Shi et al. 2004; Forneris et al. 2005). We hypothesize that one possible reason why neuroLSD1^{KO} mice are protected against seizure is because REST-repressive activity is strengthened in the brain when LSD1 dominant-negative isoform, neuroLSD1, is absent (Zibetti et al. 2010; Toffolo et al. 2014). Consistently, it has been demonstrated that boosting REST-mediated repression prevents epilepsy. Indeed, it has been shown that

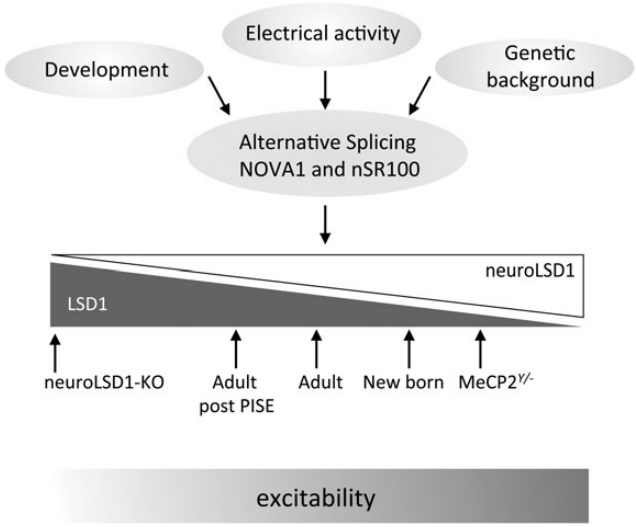

Figure 8. Model linking development, electrical activity and genetic background to excitability through modification of LSD1-related gene transcription (Toffolo et al. 2014). In the mammalian brain ratio between LSD1 and neuroLSD1 is controlled by the neurospecific splicing factors NOVA1 and nSR100 and correlates with neuronal excitability. Different LSD1/neuroLSD1 conditions are indicated.

administering a ketogenic diet or a pharmacological treatment with 2-deoxiglucose (a widely used therapeutic approach to epilepsy) increases REST binding to CtBP, a member of the LSD1/CoREST co-repressor complex (Garriga-Canut et al. 2006). Interestingly, in the brain, the splicing factor nSR100 is known to control also REST4, a REST dominant-negative isoform (Raj et al. 2011), suggesting that nSR100, by regulating alternative splicing of both neuroLSD1 and the dominant-negative isoform REST4, regulates REST-mediated gene repression through converging strategies.

To summarize, we delineate a picture where NOVA1 and nSR100 modulate in a concerted way LSD1/neuroLSD1 as well as the REST/REST4 (Raj et al. 2011) ratios in the brain, contributing to homeostatically reset transcription to modify the excitability threshold in response to seizures (Fig. 8). Clinical perspectives entail the possibility to modulate neurospecific splicing of LSD1 to treat hyperexcitability-associated neurological disorders including RTT. In addition, it could be interesting to investigate whether basal LSD1/neuroLSD1 ratios vary depending on the genetic background, possibly predisposing to or protecting from specific pathological conditions associated with alterations of the cerebral E/I ratio including epilepsy.

Supplementary Material

Supplementary can be found at: http://www.cercor.oxfordjournals.org/.

Funding

This work was supported by the Epigenomics Flagship Project EPIGEN (MIUR-CNR) (E.B.), Fondazione Cariplo Projects 2009-2640 (E.B.); "Dote ricerca": FSE, Regione Lombardia (F.R.); Jerome Lejeune Foundation (N.L,); Telethon (Grant GGP10032 to N.L.); Ministero della Salute (Ricerca finalizzata 2008–Bando Malattie Rare to N.L.); and proRETT ricerca. L.Pa and L.Po. are supported by Fondazione Fratelli Confalonieri.

Notes

We are very grateful to Maria Estela Andrès, Riccardo Brambilla, and Beatrice Bodega for their stimulating discussions, Susanna Terzano for critical revision of the manuscript and Barbara Grillo and Lucia Romanelli for technical contribution. *Conflict of Interest:* None declared.

References

Adamo A, Barrero MJ, Izpisua Belmonte JC. 2011. LSD1 and pluripotency: a new player in the network. Cell Cycle. 10:3215–3216.
Baralle D, Baralle M. 2005. Splicing in action: assessing disease causing sequence changes. J Med Genet. 42:737–748.
Baralle M, Baralle D, De Conti L, Mattocks C, Whittaker J, Knezevich A, Ffrench-Constant C, Baralle FE. 2003. Identification of a mutation that perturbs NF1 agene splicing using genomic DNA samples and a minigene assay. J Med Genet. 40:220–222.
Ben-Shachar S, Chahrour M, Thaller C, Shaw CA, Zoghbi HY. 2009. Mouse models of MeCP2 disorders share gene expression changes in the cerebellum and hypothalamus. Hum Mol Genet. 18:2431–2442.
Boutz PL, Stoilov P, Li Q, Lin CH, Chawla G, Ostrow K, Shiue L, Ares M, Black DL. 2007. A post-transcriptional regulatory switch in polypyrimidine tract-binding proteins reprograms alternative splicing in developing neurons. Genes Dev. 21:1636–1652.
Braunschweig U, Gueroussov S, Plocik AM, Graveley BR, Blencowe BJ. 2013. Dynamic integration of splicing within gene regulatory pathways. Cell. 152:1252–1269.
Calarco JA, Superina S, O'Hanlon D, Gabut M, Raj B, Pan Q, Skalska U, Clarke L, Gelinas D, van der Kooy D et al. 2009. Regulation of vertebrate nervous system alternative splicing and development by an SR-related protein. Cell. 138:898–910.
Chahrour M, Jung SY, Shaw C, Zhou X, Wong ST, Qin J, Zoghbi HY. 2008. MeCP2, a key contributor to neurological disease, activates and represses transcription. Science. 320:1224–1229.
Chahrour M, Zoghbi HY. 2007. The story of Rett syndrome: from clinic to neurobiology. Neuron. 56:422–437.
Dolce A, Ben-Zeev B, Naidu S, Kossoff EH. 2013. Rett syndrome and epilepsy: an update for child neurologists. Pediatr Neurol. 48:337–345.
Ellis JD, Barrios-Rodiles M, Colak R, Irimia M, Kim T, Calarco JA, Wang X, Pan Q, O'Hanlon D, Kim PM et al. 2012. Tissue-specific alternative splicing remodels protein-protein interaction networks. Mol Cell. 46:884–892.
Eom T, Zhang C, Wang H, Lay K, Fak J, Noebels JL, Darnell RB. 2013. NOVA-dependent regulation of cryptic NMD exons controls synaptic protein levels after seizure. Elife. 2:e00178.
Forneris F, Binda C, Vanoni MA, Battaglioli E, Mattevi A. 2005. Human histone demethylase LSD1 reads the histone code. J Biol Chem. 280:41360–41365.
Garriga-Canut M, Schoenike B, Qazi R, Bergendahl K, Daley TJ, Pfender RM, Morrison JF, Ockuly J, Stafstrom C, Sutula T et al. 2006. 2-Deoxy-D-glucose reduces epilepsy progression by NRSF-CtBP-dependent metabolic regulation of chromatin structure. Nat Neurosci. 9:1382–1387.
Guy J, Cheval H, Selfridge J, Bird A. 2011. The role of MeCP2 in the brain. Annu Rev Cell Dev Biol. 27:631–652.
Guy J, Hendrich B, Holmes M, Martin JE, Bird A. 2001. A mouse Mecp2-null mutation causes neurological symptoms that mimic Rett syndrome. Nat Genet. 27:322–326.
Irimia M, Blencowe BJ. 2012. Alternative splicing: decoding an expansive regulatory layer. Curr Opin Cell Biol. 24:323–332.
Jelen N, Ule J, Zivin M. 2010. Cholinergic regulation of striatal Nova mRNAs. Neuroscience. 169:619–627.
Kalsotra A, Cooper TA. 2011. Functional consequences of developmentally regulated alternative splicing. Nat Rev Genet. 12:715–729.
Lee JA, Tang ZZ, Black DL. 2009. An inducible change in Fox-1/A2BP1 splicing modulates the alternative splicing of downstream neuronal target exons. Genes Dev. 23:2284–2293.
Li Q, Lee JA, Black DL. 2007. Neuronal regulation of alternative pre-mRNA splicing. Nat Rev Neurosci. 8:819–831.
Licatalosi DD, Darnell RB. 2010. RNA processing and its regulation: global insights into biological networks. Nat Rev Genet. 11:75–87.

Lipscombe D. 2005. Neuronal proteins custom designed by alternative splicing. Curr Opin Neurobiol. 15:358–363.
Liu P, Jenkins NA, Copeland NG. 2003. A highly efficient recombineering-based method for generating conditional knockout mutations. Genome Res. 13:476–484.
McKee AE, Silver PA. 2007. Systems perspectives on mRNA processing. Cell Res. 17:581–590.
Nakano Y, Jahan I, Bonde G, Sun X, Hildebrand MS, Engelhardt JF, Smith RJ, Cornell RA, Fritzsch B, Bánfi B. 2012. A mutation in the Srrm4 gene causes alternative splicing defects and deafness in the Bronx waltzer mouse. PLoS Genet. 8:e1002966.
Nan X, Bird A. 2001. The biological functions of the methyl-CpG-binding protein MeCP2 and its implication in Rett syndrome. Brain Dev. 23(Suppl 1):S32–S37.
Racine R, Okujava V, Chipashvili S. 1972. Modification of seizure activity by electrical stimulation. 3. Mechanisms. Electroencephalogr Clin Neurophysiol. 32:295–299.
Raj B, O'Hanlon D, Vessey JP, Pan Q, Ray D, Buckley NJ, Miller FD, Blencowe BJ. 2011. Cross-regulation between an alternative splicing activator and a transcription repressor controls neurogenesis. Mol Cell. 43:843–850.
Roopra A, Dingledine R, Hsieh J. 2012. Epigenetics and epilepsy. Epilepsia. 53 (Suppl 9):2–10.
Rusconi F, Mancinelli E, Colombo G, Cardani R, Da Riva L, Bongarzone I, Meola G, Zippel R. 2010. Proteome profile in Myotonic Dystrophy type 2 myotubes reveals dysfunction in protein processing and mitochondrial pathways. Neurobiol Dis. 38:273–280.
Skene PJ, Illingworth RS, Webb S, Kerr AR, James KD, Turner DJ, Andrews R, Bird AP. 2010. Neuronal MeCP2 is expressed at near histone-octamer levels and globally alters the chromatin state. Mol Cell. 37:457–468.
Sharma AK, Reams RY, Jordan WH, Miller MA, Thacker HL, Snyder PW. 2007. Mesial temporal lobe epilepsy: pathogenesis, induced rodent models and lesions. Toxicol Pathol. 35:984–999.
Shepherd GM, Katz DM. 2011. Synaptic microcircuit dysfunction in genetic models of neurodevelopmental disorders: focus on Mecp2 and Met. Curr Opin Neurobiol. 21:827–833.
Shi Y, Lan F, Matson C, Mulligan P, Whetstine JR, Cole PA, Casero RA. 2004. Histone demethylation mediated by the nuclear amine oxidase homolog LSD1. Cell. 119:941–953.
Shibley H, Smith BN. 2002. Pilocarpine-induced status epilepticus results in mossy fiber sprouting and spontaneous seizures in C57BL/6 and CD-1 mice. Epilepsy Res. 49:109–120.
Stojic L, Jasencakova Z, Prezioso C, Stützer A, Bodega B, Pasini D, Klingberg R, Mozzetta C, Margueron R, Puri PL et al. 2011. Chromatin regulated interchange between polycomb repressive complex 2 (PRC2)-Ezh2 and PRC2-Ezh1 complexes controls myogenin activation in skeletal muscle cells. Epigenetics Chromatin. 4:16.
Toffolo E, Rusconi F, Paganini L, Tortorici M, Pilotto S, Heise C, Verpelli C, Tedeschi G, Maffioli E, Sala C et al. 2014. Phosphorylation of neuronal lysine-specific demethylase 1LSD1/KDM1A impairs transcriptional repression by regulating interaction with CoREST and histone deacetylases HDAC1/2. J Neurochem. 128: 603–616.
Ule J, Darnell RB. 2006. RNA binding proteins and the regulation of neuronal synaptic plasticity. Curr Opin Neurobiol. 16:102–110.
Zhang C, Frias MA, Mele A, Ruggiu M, Eom T, Marney CB, Wang H, Licatalosi DD, Fak JJ, Darnell RB. 2010. Integrative modeling defines the Nova splicing-regulatory network and its combinatorial controls. Science. 329:439–443.
Zhang L, He J, Jugloff DG, Eubanks JH. 2008. The MeCP2-null mouse hippocampus displays altered basal inhibitory rhythms and is prone to hyperexcitability. Hippocampus. 18:294–309.
Zibetti C, Adamo A, Binda C, Forneris F, Toffolo E, Verpelli C, Ginelli E, Mattevi A, Sala C, Battaglioli E. 2010. Alternative splicing of the histone demethylase LSD1/KDM1 contributes to the modulation of neurite morphogenesis in the mammalian nervous system. J Neurosci. 30:2521–2532.